

# Hadron Spectrum in QCD with Valence Wilson Fermions and Dynamical Staggered Fermions at $6/g^2 = 5.6$

Khalil M. Bitar, R.G. Edwards, U.M. Heller, A.D. Kennedy  
*SCRI, The Florida State University, Tallahassee, FL 32306-4052, USA*

Thomas A. DeGrand  
*Physics Department, University of Colorado, Boulder, CO 80309, USA*

Steven Gottlieb, A. Krasnitz  
*Department of Physics, Indiana University, Bloomington, IN 47405, USA*

J. B. Kogut  
*Department of Physics  
University of Illinois, 1110 W. Green St., Urbana, IL 61801, USA*

W. Liu, Pietro Rossi  
*Thinking Machines Corporation, Cambridge, Mass. 02142, USA*

Michael C. Ogilvie  
*Department of Physics, Washington University, St. Louis, MO 63130, USA*

R. L. Renken  
*Department of Physics, University of Central Florida, Orlando, FL 32816, USA*

D. K. Sinclair  
*HEP Division  
Argonne National Laboratory, 9700 S. Cass Ave., Argonne, IL 60439, USA*

R. L. Sugar  
*Department of Physics, University of California, Santa Barbara, CA 93106, USA*

D. Toussaint  
*Department of Physics, University of Arizona, Tucson, AZ 85721, USA*

K. C. Wang  
*Department of Physics, University of New South Wales, Kensington, NSW 2203, Australia*

### **Abstract**

We present an analysis of hadronic spectroscopy for Wilson valence quarks with dynamical staggered fermions at lattice coupling  $6/g^2 = \beta = 5.6$  at sea quark mass  $am_q = 0.01$  and  $0.025$ , and of Wilson valence quarks in quenched approximation at  $\beta = 5.85$  and  $5.95$ , both on  $16^3 \times 32$  lattices. We make comparisons with our previous results with dynamical staggered fermions at the same parameter values but on  $16^4$  lattices doubled in the temporal direction.

# 1 Introduction

Calculations of hadron spectroscopy remain an important part of nonperturbative studies of QCD using lattice methods. (For a review of recent progress in this field, see Ref. [1].) We have been engaged in an extended program of calculation of the masses and other parameters of the light hadrons in simulations which include the effects of two flavors of light dynamical quarks. These quarks are realized on the lattice as staggered fermions. We have carried out simulations with lattice valence quarks in both the staggered and Wilson formulations. Our reasons for performing simulations with Wilson valence quarks is twofold: First, we are interested in seeing if there are any effects of sea quarks on the spectroscopy of systems containing either realization of valence quark. Thus this work complements our parallel studies of spectroscopy with staggered valence and sea quarks, and of spectroscopy with Wilson valence and sea quarks. Second, we are interested in exploring the effects of sea quarks on simple matrix elements such as the pseudoscalar meson decay constant. Most previous work has been done with Wilson valence quarks in quenched approximation. We consider that mixing the two realizations is not inappropriate for a first round of numerical simulations.

These simulations are performed on  $16^3 \times 32$  lattices at lattice coupling  $6/g^2 = \beta = 5.6$  with two masses of dynamical staggered fermions,  $am_q = 0.025$  and  $am_q = 0.01$ . These are the same parameter values as we used in our first round of simulations[2] However, the first set of simulations have two known inadequacies. The first is that most of our runs were carried out on lattices of spatial size  $12^3$ . A short run on  $16^3$  lattices with dynamical quark mass 0.01 showed that these lattices were too small: baryon masses fell by about fifteen per cent on the larger lattice compared to the smaller one. Thus the  $am_q = 0.025$  results from Ref. [2] are suspect and need to be redone. We also felt that we needed more statistics on the  $am_q = 0.01$  system.

Second, nearly all of our running was done on lattices of size  $12^4$  or  $16^4$ ; these lattices were doubled in the temporal direction to  $12^3 \times 24$  or  $16^3 \times 32$  for spectroscopy studies. Doubling the lattice introduced strange structure in the propagators of some of the particles: the pion mass, in particular, showed strange oscillatory behavior as a function of position on the lattice. This behavior is almost certainly due to doubling the lattice[3] and the best way to avoid this problem is to begin with a larger lattice in the temporal direction.

Finally, it is an open question how much sea quarks affect the hadronic spectrum. In order to address this question, we have performed a set of simulations in the quenched approximation at lattice couplings  $\beta = 5.85$  and  $5.95$ , also on  $16^3 \times 32$  lattices. As the reader will see, our quenched results are rather similar to our results with dynamic fermions; apparently at the particular values of sea quark mass and lattice coupling where our simulations were performed, the effects of sea quarks can be absorbed into renormalizations of the lattice coupling and valence quark mass.

Some of the results described here have been presented in preliminary form in Ref. [4]. Several other papers which we are preparing for publication complement the results presented here: we are also preparing a paper on spectroscopy results with valence staggered quarks, an analysis of simple matrix elements with Wilson

valence quarks, a study of valence quark Coulomb gauge wave functions, and a study of glueballs and topology in the presence of dynamical staggered quarks.

## 2 The simulations

Our simulations were performed on the Connection Machine CM-2 located at the Supercomputer Computations Research Institute at Florida State University.

We carried out simulations with two flavors of dynamical staggered quarks using the Hybrid Molecular Dynamics algorithm[5] The lattice size is  $16^3 \times 32$  sites and the lattice coupling  $\beta = 5.6$ . The dynamical quark mass is  $am_q = 0.01$  and  $0.025$ . The total simulation length was 2000 simulation time units (with the normalization of Ref. [2]) at each quark mass value, after thermalization. The  $am_q = 0.01$  run started from an equilibrated  $16^4$  lattice of our previous runs on the ETA-10, that was doubled in the time direction and then re-equilibrated for 150 trajectories. The  $am_q = 0.025$  run was started from the last configuration of the smaller mass run, and then thermalized for 300 trajectories. We recorded lattices for the reconstruction of spectroscopy every 20 HMD time units, for a total of 100 lattices at each mass value.

We computed spectroscopy with staggered sea quarks at five values of the Wilson quark hopping parameter:  $\kappa = 0.1600, 0.1585, 0.1565, 0.1525, 0.1410$ , and  $0.1320$ . The first three values are rather light quarks (the pseudoscalar mass in lattice units ranges from about 0.25 to 0.45) and the other three values correspond to heavy quarks (pseudoscalar masses of 0.65 to 1.5). The first three values are the ones we used in our first round of experiments. We computed masses of mesons with all possible combinations of quark and antiquark mass; we only computed the masses of baryons made of degenerate mass quarks.

The quenched simulations were performed at lattice couplings of  $\beta = 5.85$  and  $5.95$ , also on  $16^3 \times 32$  lattices. They used the Hybrid Monte Carlo algorithm[6] These simulations had a total length of 3200 time units at  $\beta = 5.85$  and 3800 time units at  $\beta = 5.95$ . We recorded lattices for Wilson valence spectroscopy every 40 time units, for a sample of about 90 lattices at each coupling. Our quenched spectroscopy was done at hopping parameter values designed to reproduce as accurately as possible our earlier  $\beta = 5.6$  running: we used  $\kappa = 0.1585$  and  $0.1600$  at  $\beta = 5.85$  and  $\kappa = 0.1554$  and  $0.1567$  at  $\beta = 5.95$ . We only computed spectroscopy for hadrons with degenerate quarks.

For the spectroscopy we used periodic boundary conditions in all four directions of the lattice. Our lattices are long enough in the time direction and our interpolating fields are good enough that we are always able to extract an asymptotic mass. The use of open boundary conditions introduces edge effects which are hard to quantify and we have chosen to avoid them in the current round of simulations.

We calculated hadron propagators in the following way: We fix gauge in each configuration in the data set to lattice Coulomb gauge using an overrelaxation algorithm[7] and use sources for the quarks which spread out in space uniformly over the simulation volume and restricted to a single time slice ( "wall" sources[8]). This source is nonzero only on sites which form one checkerboard of the lattice (the sum of  $x$

plus  $y$  plus  $z$  coordinates is an even number). Our inversion technique is conjugate gradient with preconditioning via ILU decomposition by checkerboards[9]. We used a fast matrix inverter written in CMIS (Connection Machine Instruction Set)[10].

We use both a spread out sink as well as a “pointlike” sink where all the quarks lines end on the same site. The “wall” sink is identical to the source, but sums over all sites. We label hadron propagators with wall sources and point sinks as “WP” and those with a wall source and a wall sink as “WW”. We combine the quark propagators into hadron propagators in an entirely conventional manner. For Wilson hadrons we use relativistic wave functions[11]. The baryon wave functions are:

Proton:

$$\begin{aligned} |P, s\rangle &= (uC\gamma_5d)u_s \\ &= (u_1d_2 - u_2d_1 + u_3d_4 - u_4d_3)u_s \end{aligned}$$

Delta:

$$\begin{aligned} |\Delta_1, s\rangle &= (u_1d_2 + u_2d_1 + u_3d_4 + u_4d_3)u_s \\ |\Delta_2, s\rangle &= (u_1d_3 - u_2d_4 + u_3d_1 - u_4d_2)u_s \end{aligned} \tag{1}$$

We have measured meson correlation functions using spin structures  $\bar{\psi}\gamma_5\psi$  and  $\bar{\psi}\gamma_0\gamma_5\psi$  for the pion and  $\bar{\psi}\gamma_3\psi$  and  $\bar{\psi}\gamma_0\gamma_3\psi$  for the rho, which we refer to as “kind = 1” and “kind = 2” for the pseudoscalar and vector, respectively.

To extract masses from the hadron propagators, we must average the propagators over the ensemble of gauge configurations, estimate the covariance matrix and use a fitting routine to get an estimate of the model parameters. The lattices used for Wilson spectroscopy with staggered sea quarks are separated by 20 HMD time units and do not show any discernable time correlations with each other. The quenched simulations, spaced 40 Hybrid Monte Carlo time units apart, show some residual time correlation when we compare the error on the pion effective mass blocking various numbers of successive lattices together. We attempt to take these correlations into effect by blocking three successive lattices together before fitting the data.

We use the full covariance matrix in fitting the propagators in order to get a meaningful estimate of the goodness of fit. Reference[12] discusses this fitting procedure in detail.

### 3 Spectroscopy Results

We determined hadron masses by fitting our data under the assumption that there was a single particle in each channel. This corresponds to fitting for one decaying exponential and its periodic partner. We calculated effective masses by fitting two successive distances, and also made fits to the propagators over larger distance ranges.

In selecting the distance range to be used in the fitting, we have tried to be systematic. We somewhat arbitrarily choose the best fitting range as the range which maximizes the confidence level of the fit (to emphasize good fits) times the number of degrees of freedom (to emphasize fits over big distance ranges) divided by the statistical error on the mass (to emphasize fits with small errors). We typically

restrict this selection to fits beginning no more than 11 or 12 timeslices from the origin.

### 3.1 Simulations with sea quarks

We computed spectroscopy for the six possible values of valence quark hopping parameter given above, with both ‘WP’ and ‘WW’ correlation functions. We first show the global results to spectroscopy, giving the best-fit value for the mass for each value of hopping parameters. We display masses as a function of the average hopping parameter  $\frac{1}{2}(\kappa_1 + \kappa_2)$  for mesons and as a function of  $\kappa$  for baryons (recall that for each sea quark mass we only studied baryons in which all three quarks have the same mass) in Figs. 1–4. In all these figures masses are quoted in lattice units. We display plots of effective mass in Fig. 5 and of mass versus  $D_{min}$  (with  $D_{max} = 16$ ) for  $\kappa = .1600$  data in Fig. 6. Since the “kind=1” and “kind=2” operators produce essentially identical spectroscopy we only show “kind=1” results in these figures in an attempt to avoid clutter. Best fit values for each particle are shown in Tables 1–8.

For all but two cases the fitting was straightforward. However, we had two difficult data sets,  $\kappa = .1320$  spectroscopy and the  $am_q = 0.01$ ,  $\kappa = .1600$  delta.

For all particles except those containing one or more of the heaviest quarks both kinds of correlation functions give consistent results, with the ‘WP’ correlators typically showing the smallest uncertainty. For mesons or baryons containing a heavy  $\kappa = .1320$  quark, however, the ‘WP’ fits do not settle down to an asymptotic value. The effective mass drifts continuously with  $t$  value and fits to a range have unacceptably high chi-squared’s. The ‘WW’ fits are more acceptable (have a chi-squared near one per degree of freedom). Possibly what is happening is this: For these states the wall source has poor overlap on the lightest hadron in a channel, since bound states of heavy quarks have small spatial extent. The WP correlators do not give a variational bound and it happens that they approach an asymptotic mass from below. The WW correlators approach an asymptotic value from above, but are noisier; one gets a statistically more acceptable fit because of larger uncertainties on the individual points. As an example, we show effective masses as a function of  $t$  for the  $ma = 0.01$ ,  $\kappa = 0.1320$  data in Fig. 7.

Next, the  $am = 0.01$ ,  $\kappa = .1600$  delta mass is considerably lighter than we saw in our old running and nearly degenerate with the nucleon. At this light valence quark mass the ‘WW’ operators are so noisy that they are useless, but the same behavior is seen in ‘WP’ delta operators with both spin structures of Eqn. 1. A comparison of the two operators is shown in Fig. 5d (effective masses) and 6d (fits to a range  $d_{min}$  to 16). The signal for a light delta appears to be stable for fit distances ranging from  $d_{min} = 4$  out to 8 or 9, and then the signal deteriorates so rapidly that we cannot trust our fits. We do not know of a reason for this effect. A coding error would mix some component of the nucleon into the delta and the asymptotic mass in the delta channel would be the nucleon’s. However, the  $am_q = 0.025$  delta is measurably heavier than the nucleon, which argues against a coding error. One should note that the ‘WP’ correlators are not variational. It is possible that we are seeing a signal attempting to approach an asymptotic value from below, which becomes lost in the

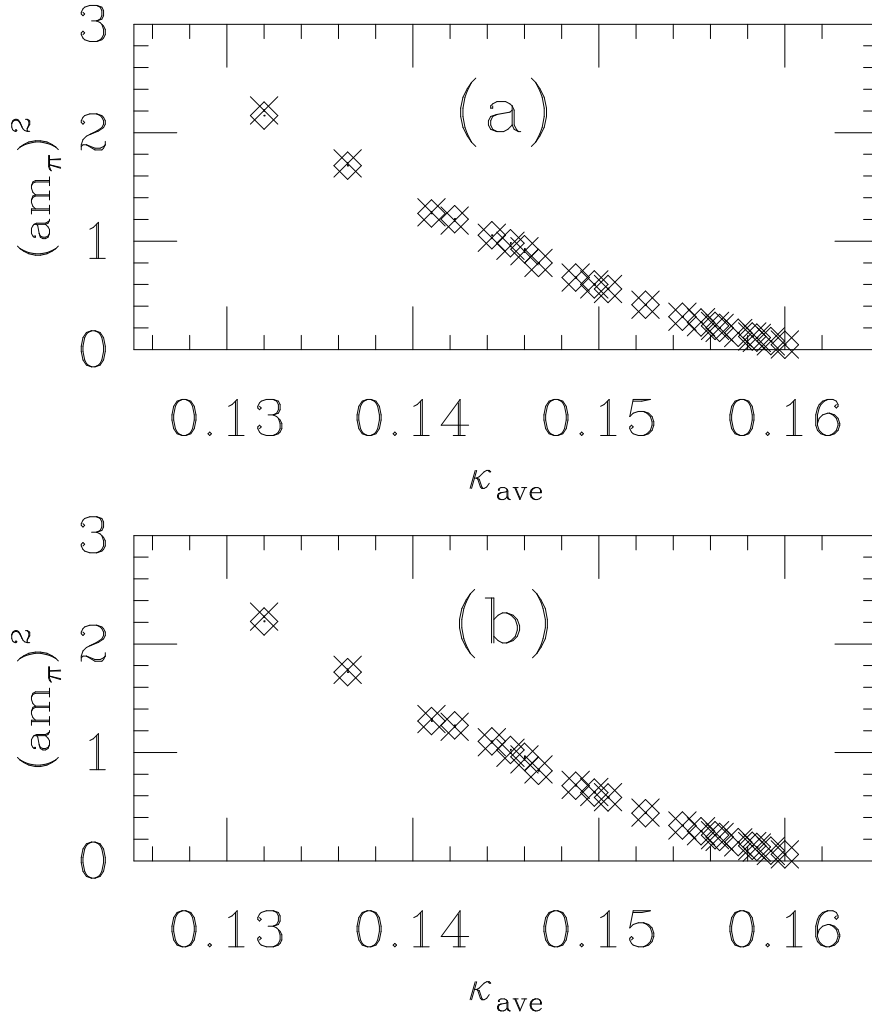


Figure 1: Best fit masses (from fits to a range) for the pseudoscalar as a function of the average hopping parameter. Data are labelled by type (WP or WW) (described in the text) by crosses (WP) and diamonds (WW). Figure (a) is for sea quark mass  $am_q = 0.01$ , (b) for  $am_q = 0.025$ .

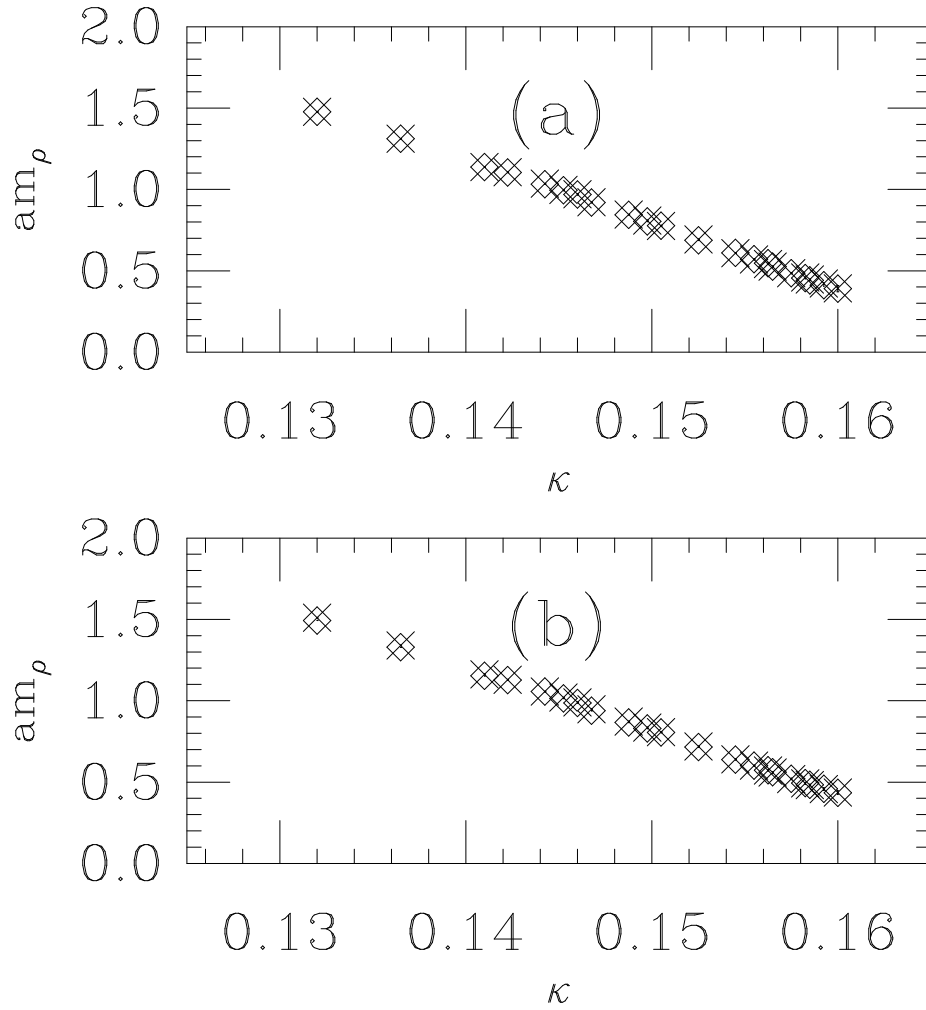


Figure 2: Best fit masses (from fits to a range) for the vector meson as a function of the average hopping parameter. Figure (a) is for sea quark mass  $am_q = 0.01$ , (b) for  $am_q = 0.025$ .



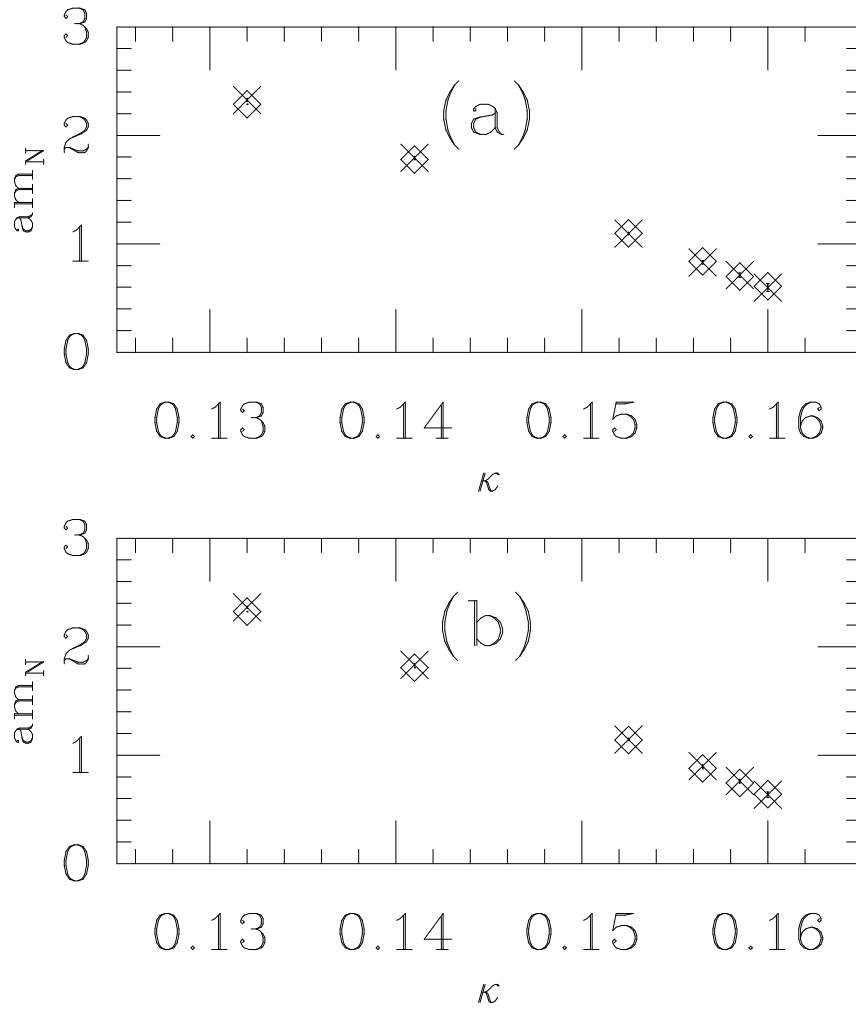


Figure 3: Best fit masses (from fits to a range) for the proton as a function of hopping parameter. Figure (a) is for sea quark mass  $am_q = 0.01$ , (b) for  $am_q = 0.025$ .

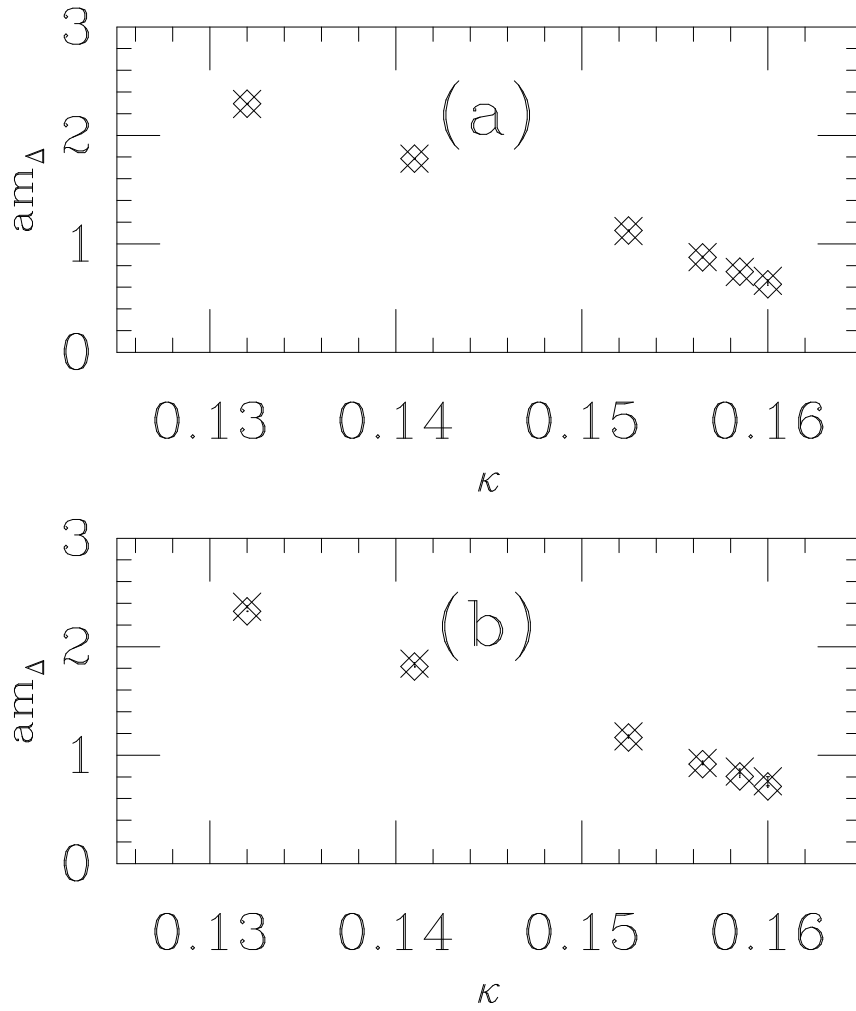


Figure 4: Best fit masses (from fits to a range) for the delta as a function of hopping parameter. Figure (a) is for sea quark mass  $am_q = 0.01$ , (b) for  $am_q = 0.025$ .

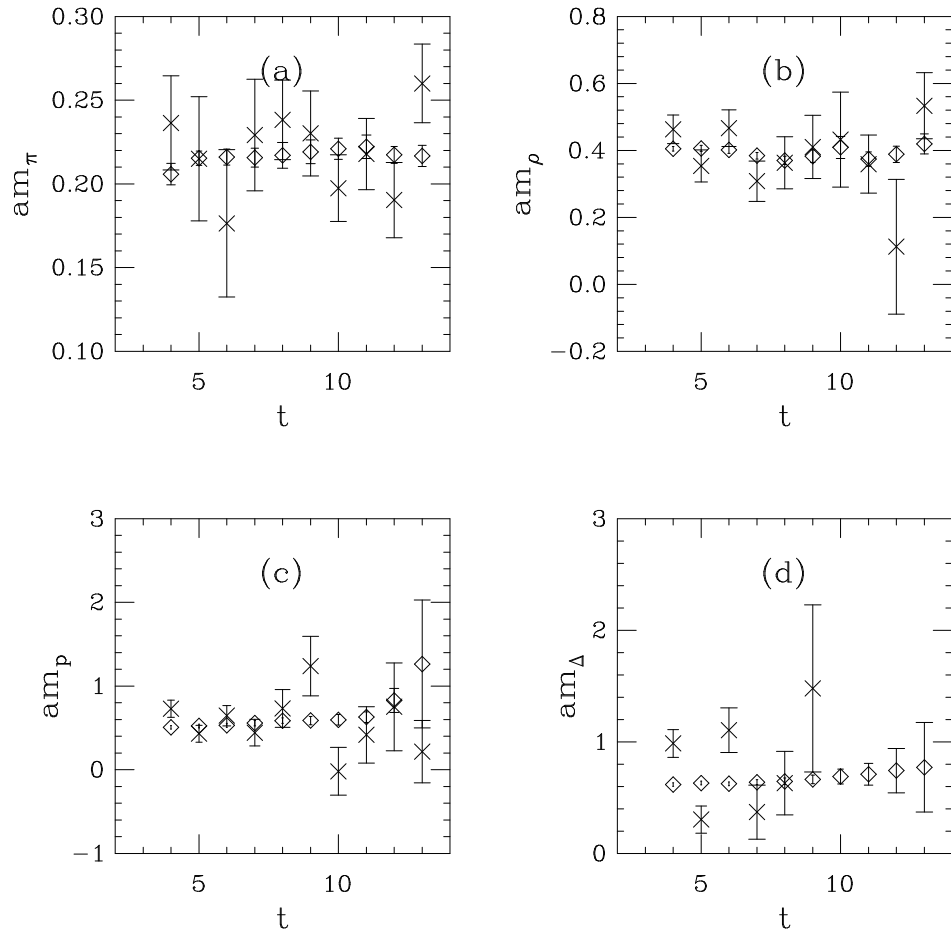


Figure 5: Effective mass fits to  $\kappa = 0.1600$  data: (a) pion, (b) rho, (c) proton, and (d) delta. Data are labelled by type (WP or WW) by crosses (WP) and diamonds (WW).

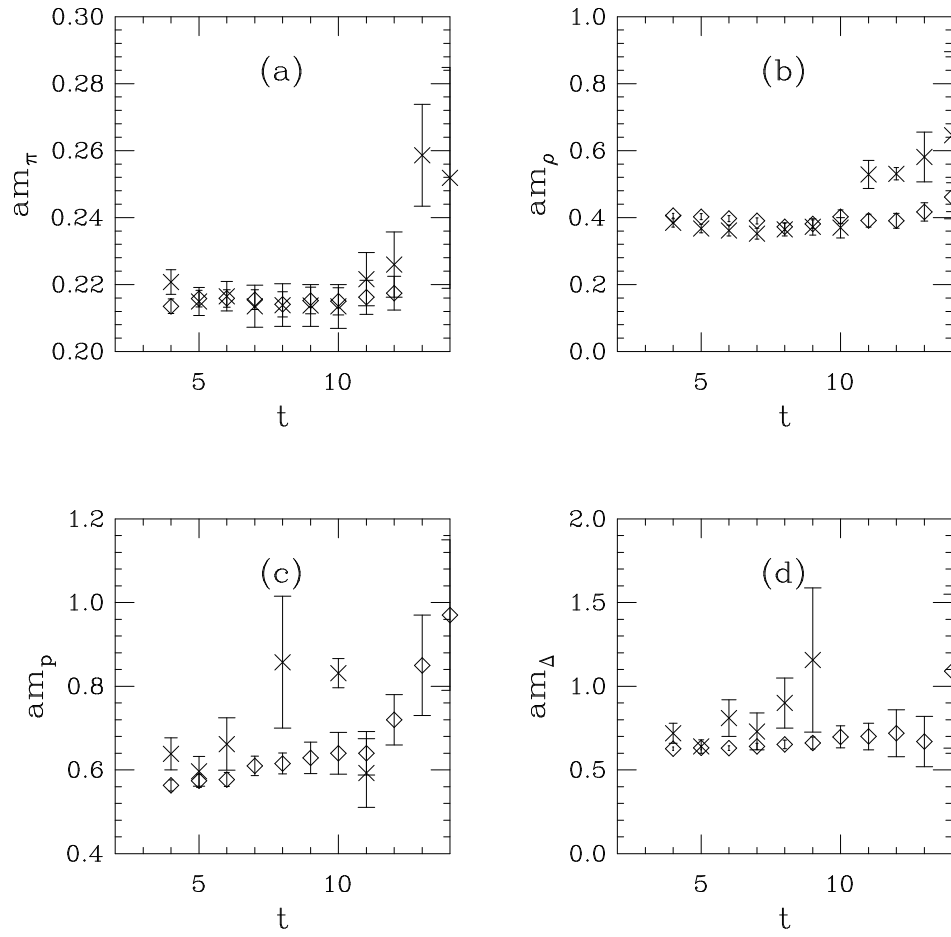


Figure 6: Fits from  $t = D_{min}$  to 16 to  $\kappa = 0.1600$  data: (a) pion, (b) rho, (c) proton, and (d) delta. Correlator types are labelled as in Fig. 1-5.

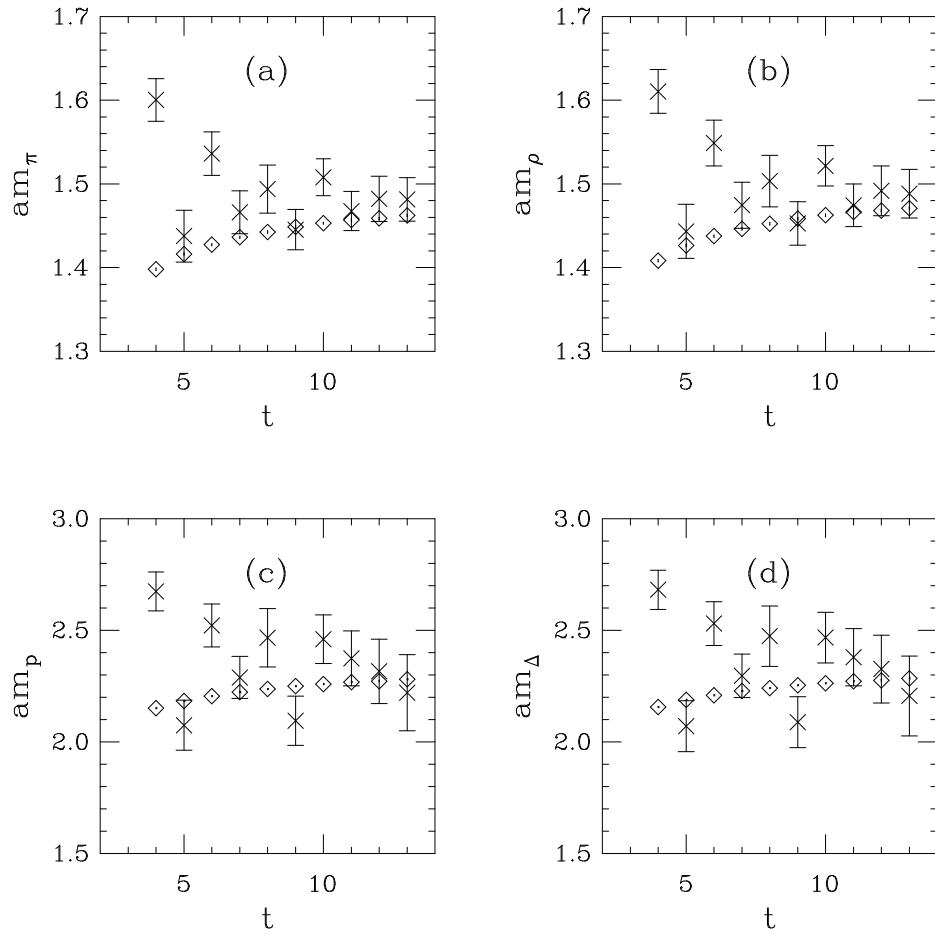


Figure 7: Effective mass fits to  $\kappa = 0.1320$  data: (a) pion, (b) rho, (c) proton, and (d) delta. Data are labelled by type (WP or WW) by crosses (WP) and diamonds (WW).

noise before its asymptotic value is reached.

Our data can be compared with our previous  $16^4$  runs: The  $\kappa = .1585$  and  $.1600$  pseudoscalar vector, and proton masses are consistent with the old numbers. The  $\kappa = .1585$  deltas are consistent but the new  $\kappa = .1600$  delta is quite a bit lighter (0.63 vs. 0.74). At  $\kappa = .1565$  we had run before only on  $12^3$  lattices. The new proton is lighter (0.84 vs. 0.89) and so is the delta (0.87 vs. 0.96). Clearly the old  $\kappa = .1565$  masses were compromised by the size of the simulation volume (as were the simulations at lighter valence quark mass). All  $am_q = 0.025$  baryons are also ten to fifteen per cent lighter than their values on  $12^3$  lattices.

We do not see any oscillations in the pion effective mass at  $\kappa = .1600$  which we saw in the old doubled  $16^4$  running (compare Fig. 5.) There, however, the effect was most dramatic for the staggered valence quark pion.

Assuming that  $m_\pi^2$  is linear in  $\kappa$  (as we expect from current algebra considerations), we can compute the critical coupling  $\kappa_c$  at which the pion becomes massless. We extrapolate using

$$(m_\pi a)^2 = A\left(\frac{1}{\kappa} - \frac{1}{\kappa_c}\right) \quad (2)$$

The fit is acceptable only for the three lightest quark masses and the final numbers are essentially unchanged whether we use all six combinations of quarks in the pseudoscalar or restrict ourselves to the three cases of degenerate quark masses. We find that  $A = 1.10(1)$  and  $\kappa_c = 0.1610(1)$  for  $am_q = 0.01$ . These numbers are in good agreement with our previous results ( $A = 1.15(16)$  and  $\kappa = 0.1611(1)$ ).

The  $am_q = 0.025$  numbers are quite different from our previous study. There we had  $A = 1.15(16)$  and  $\kappa_c = 0.1618(1)$ . Here we have  $A = 1.14(1)$ ,  $\kappa_c = 0.1613(1)$  from the 'kind=1, WP' operator,  $A = 1.17(2)$ ,  $\kappa_c = 0.1613(1)$  from the 'kind=2, WP' operator, using only equal quark mass pions. This is such a large change that it cannot be due to a statistical fluctuation. When we graph the square of the pion mass from the old simulations (on a  $12^3$  lattice) and from the new simulations (on a  $16^3$  lattice) we see that the new pions are consistently lighter than the old ones. The situation is illustrated in Fig. 8, where we also show the old and new  $am_q = 0.01$  data. It is very strange that a finite size effect (if that is what we are seeing) would be stronger for heavier dynamical fermion mass.

In Fig. 9 we present an Edinburgh plot ( $m_p/m_\rho$  vs  $m_\pi/m_\rho$ ). This figure also includes data from other simulations we have performed. Mass ratios, computed using correlated fits to a single exponential in each channel, are shown in Tables 9–12. We quantify the magnitude of hyperfine splittings in the meson and baryon sectors by comparing the two dimensionless quantities

$$R_M = \frac{m_\rho - m_\pi}{3m_\rho + m_\pi} \quad (3)$$

and

$$R_B = \frac{m_\Delta - m_p}{m_\Delta + m_p}. \quad (4)$$

Each of these quantities is the ratio of hyperfine splitting in a multiplet divided by the center of mass of the multiplet. A plot of  $R_M$  vs.  $R_B$  is shown in Fig. 10.

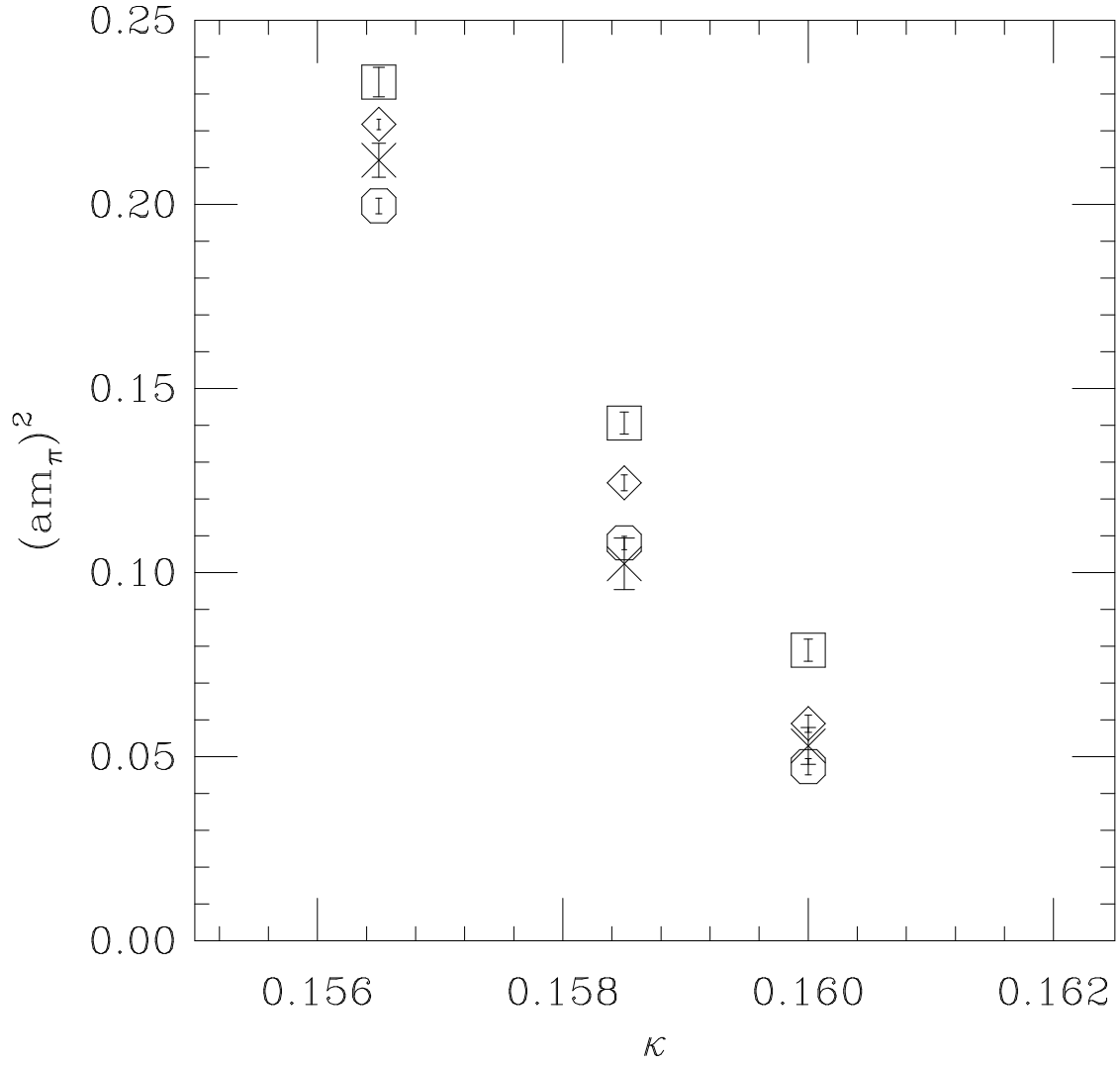


Figure 8: Square of pion mass versus hopping parameter from the old  $am_q = 0.025$  data (diamonds), new  $am_q = 0.025$  data (squares), old  $am_q = 0.01$  data (crosses) and new  $am_q = 0.01$  data (octagons)

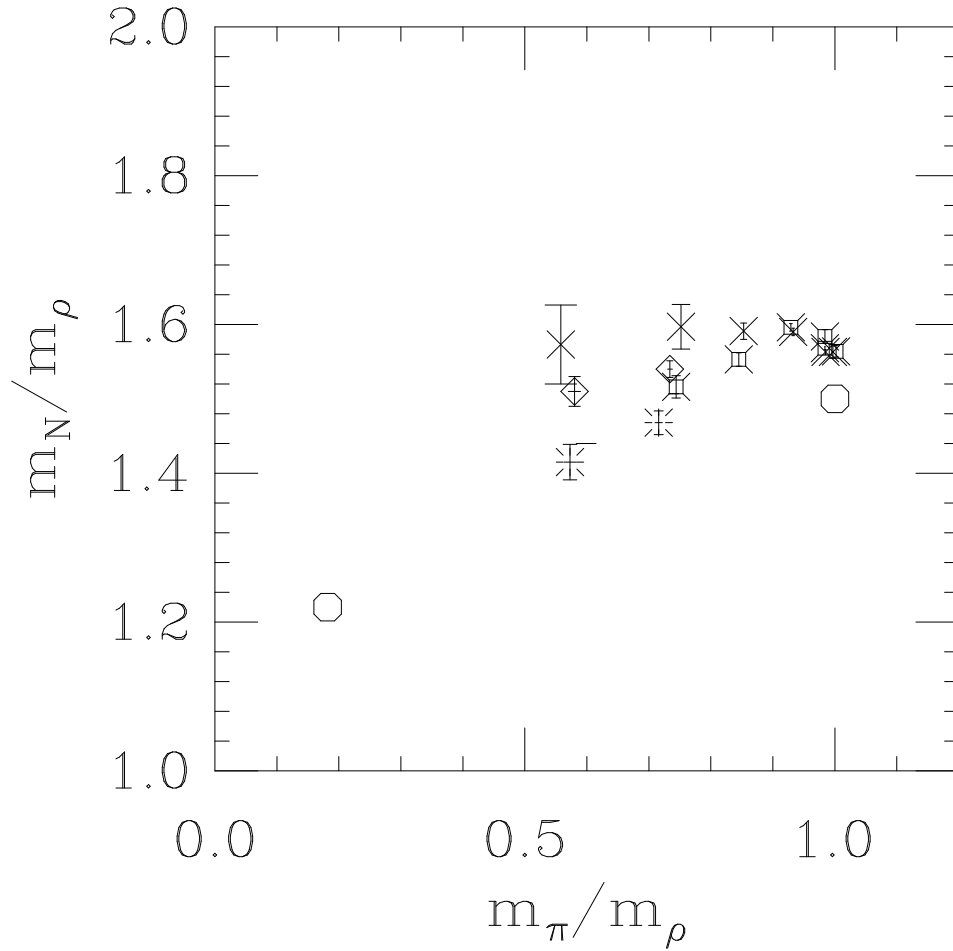


Figure 9: Edinburgh plot for Wilson valence quarks. Data are: simulations with dynamical staggered fermions at  $\beta = 5.6$  and  $am_q = 0.01$  from the  $16^4$  running (diamonds) and from the  $16^3 \times 32$  running (crosses),  $\beta = 5.6$ ,  $am_q = 0.025$   $16^3 \times 32$  simulations (fancy squares), and quenched simulations at  $\beta = 5.85$  and  $\beta = 5.95$  (bursts). The circles show the expected infinite quark mass limit and the real-world point.



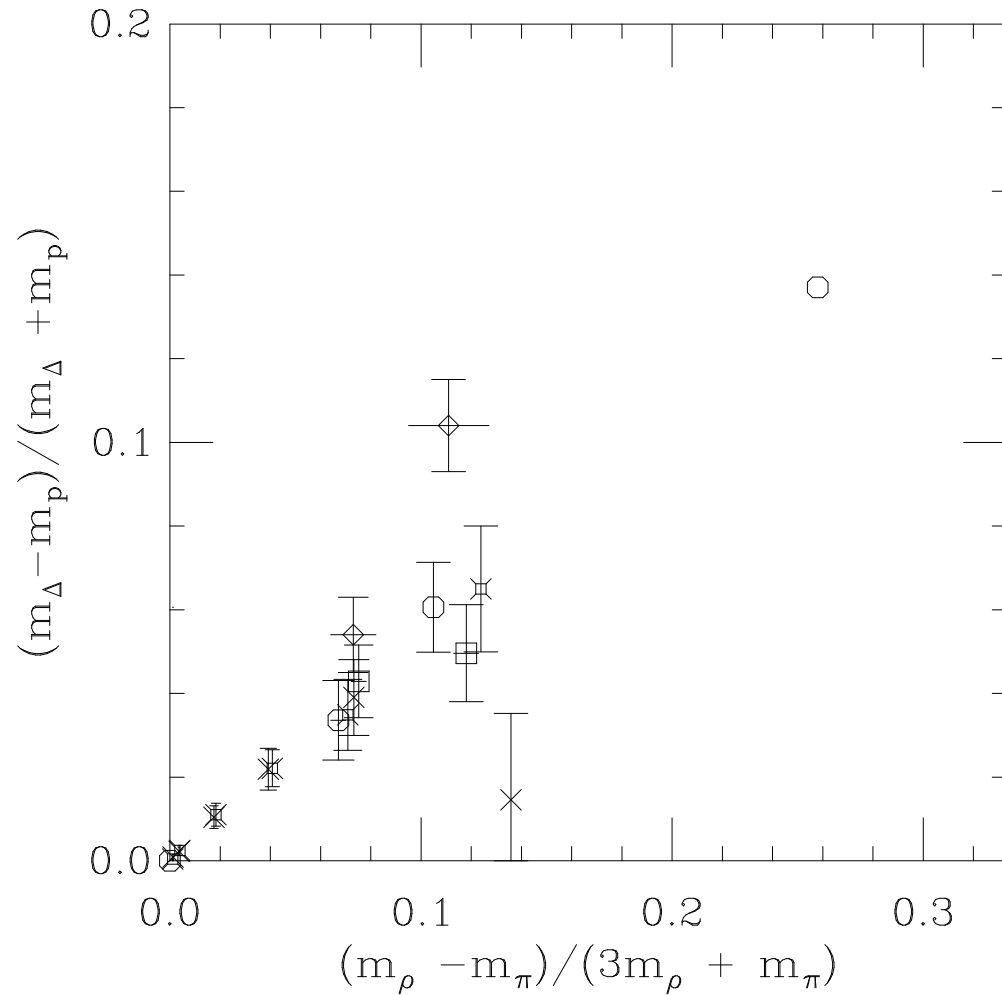


Figure 10: Comparison of baryon and meson hyperfine splitting. The two circles show the expected values of hyperfine splitting in the limit of infinite quark mass and from experiment. Points are labelled as in Fig. 9.

In the nonrelativistic quark model, the mass of a hadron is given by a sum of constituent quark masses plus a color hyperfine term,

$$M_H = \sum_i m_i + \xi_H \sum_{ij} \frac{\sigma_i \cdot \sigma_j}{m_i m_j} \quad (5)$$

where  $\xi$  is twice as great for mesons as for baryons because of color[13] From this model one expects the ratio  $R_B/R_M = 1$ . For all but the lightest quark mass data points, this is the behavior which our data shows.

If we wish to use our spectrum results to find a lattice spacing, we can extrapolate particle masses to  $\kappa_c$ , fix one mass to experiment, and use this mass to infer a lattice spacing. We can do this for the  $\rho$ , proton, and  $\Delta$  for either sea quark mass. Restricting our extrapolation to the lightest three valence hopping parameters, we display our results in Table 13. Taking the rho as the particle whose mass is forced to its physical value, we have an inverse lattice spacing of 2140 MeV or 2000 MeV, proton masses of 1121 and 1116 MeV, and deltas at 1198 and 1302 MeV. Using the proton mass to set the scale, we have inverse lattice spacings of 1800 or 1685 MeV, rhos at 648 and 650 MeV and deltas at 1008 and 1100 MeV. In all cases the proton to rho mass ratio is larger than experiment, and the proton-delta hyperfine splitting is too small.

### 3.2 Quenched Simulations

In an attempt to see whether any effects of dynamic fermions could be seen in the spectroscopy, we performed a quenched simulation with the same lattice volume as our dynamical simulations and with a large enough data set to overwhelm statistical fluctuations[4]

All fits are quite stable. We show one example of effective masses, for the  $\beta = 5.95$ ,  $\kappa = 0.1554$  data set (Fig. 11). The best fits to a range of points, selected using the histogram technique, begin at  $t_{min} = 6$  to 8, and are shown in Fig. 12 and Tables 14 and 15. Mass ratios are found in Tables 16 and 17. Our quenched data at  $\beta = 5.85$ ,  $\kappa = .1585$  are consistent within statistical errors with the earlier work of Iwasaki, et. al.[14]

While one cannot say anything about the behavior of the pion mass as a function of hopping parameter with two data points per  $\beta$  value, one can still extrapolate the square of the pion mass to zero. Doing so, we find  $\kappa_c = 0.1617(1)$ ,  $A = 1.12(4)$  for  $\beta = 5.85$  and  $\kappa_c = 0.1583(1)$ ,  $A = 1.10(3)$  for  $\beta = 5.95$ .

Finally, as a direct way of displaying any differences between our dynamical and quenched simulations, we show hadron masses (rho, proton, and delta) as a function of the pion mass in lattice units (Fig. 13). With the possible exception of the  $am_q = 0.01$ ,  $\kappa = .1600$  delta, one cannot see any strong difference between spectroscopy with or without dynamical fermions at the parameter values used in this study. There is a hint in the Edinburgh plot that the nucleon to rho mass ratio in the presence of  $am_q = 0.01$  dynamical fermions is a bit higher than in quenched approximation. We display the square of the pion mass in lattice units as a function of  $\kappa_c - \kappa$  in Fig. 14. Again all the data at the lightest valence quark masses appear to lie on a (nearly) universal curve.

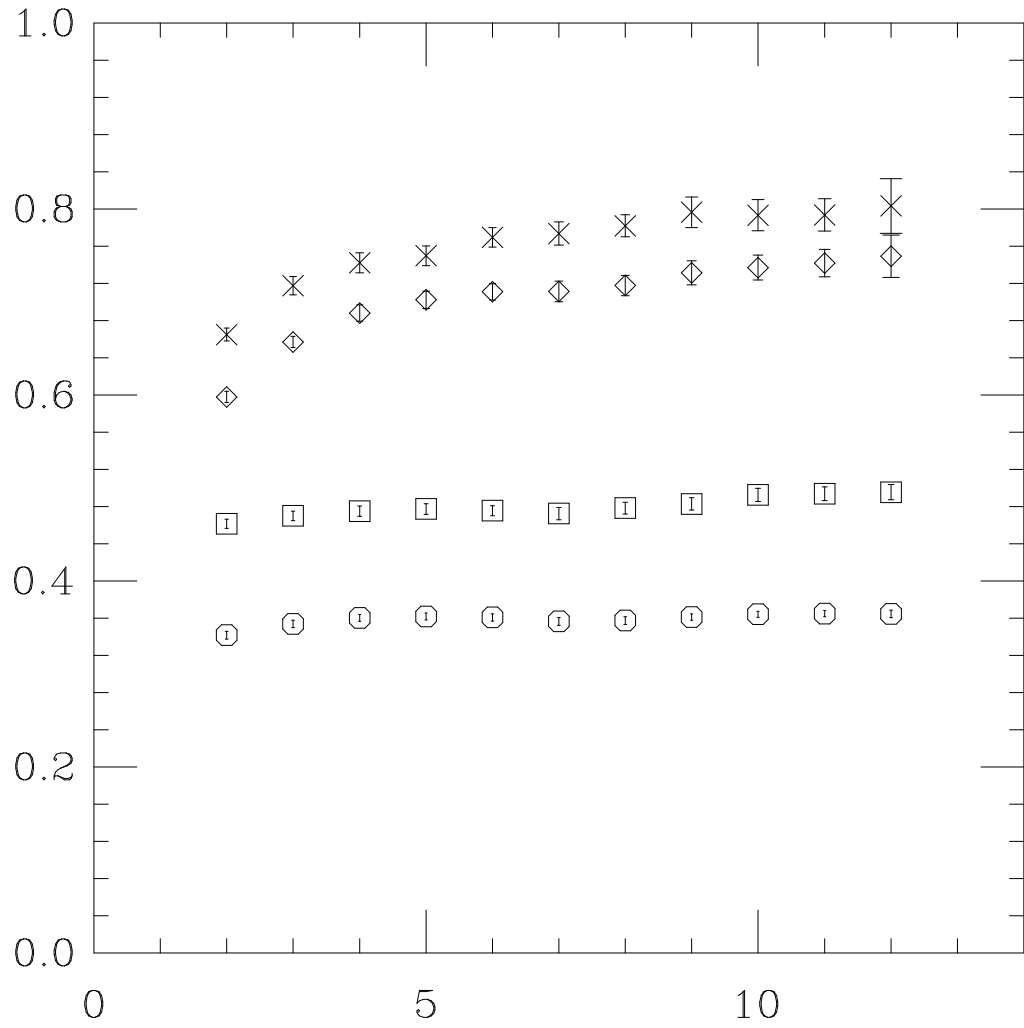


Figure 11: Effective masses from WP operators from quenched spectroscopy at  $\beta = 5.95$ ,  $\kappa = 0.1554$ . Particles in increasing order of mass are pion, rho, proton, and delta.

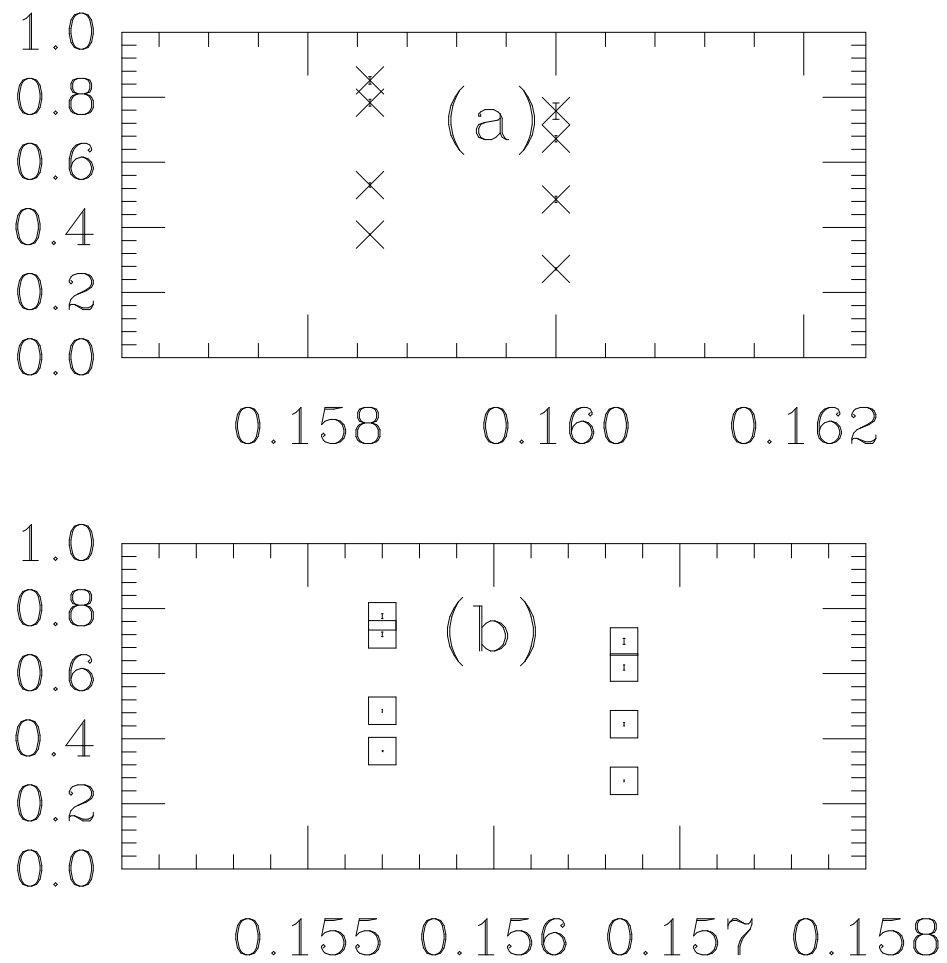


Figure 12: Quenched masses from  $\beta = 5.85$  (a) and  $\beta = 5.95$  (b) simulations. Particles in increasing order of mass are pion, rho, proton, and delta.

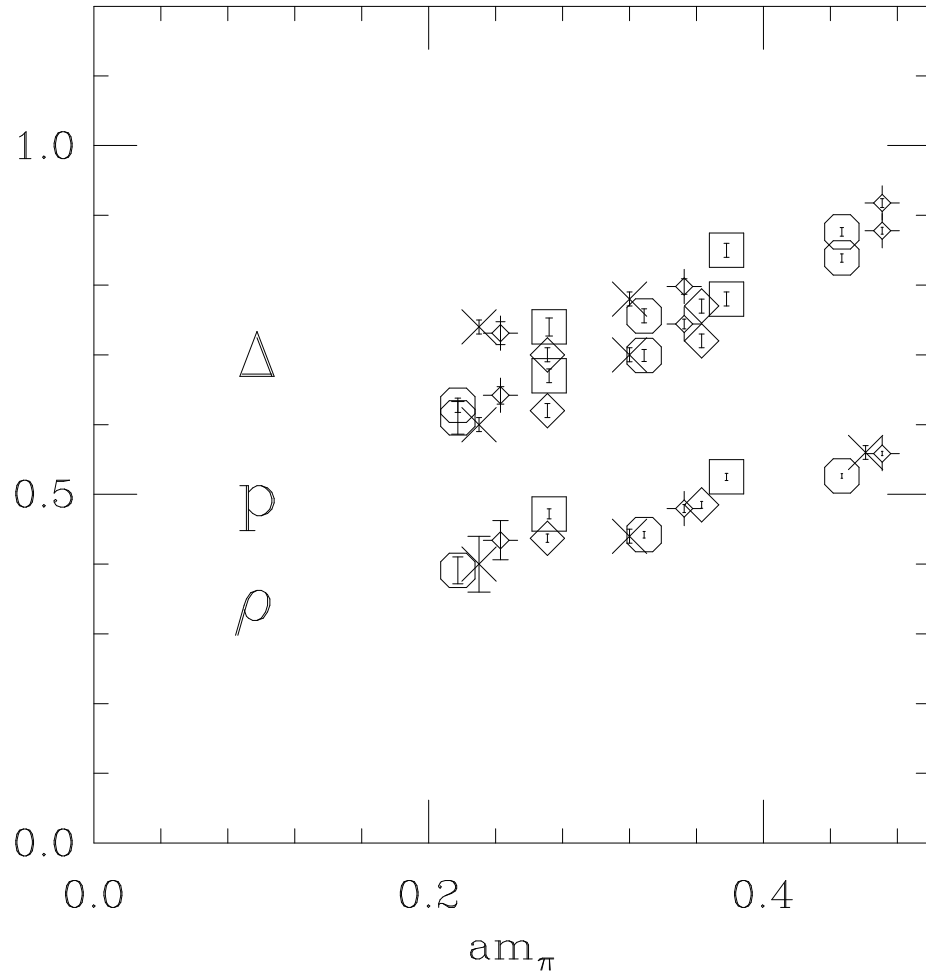


Figure 13: Hadron masses ( $\rho$ ,  $p$  and  $\Delta$ ) as a function of  $m_\pi$  for quenched and dynamical staggered simulations. Data are labelled with squares and diamonds for quenched  $\beta = 5.85$  and  $5.95$  simulations, crosses for the  $16^4$   $am_q = 0.01$  simulations, and octagons and fancy diamonds for the  $am_q = 0.01$  and  $0.025$  data presented in this paper.

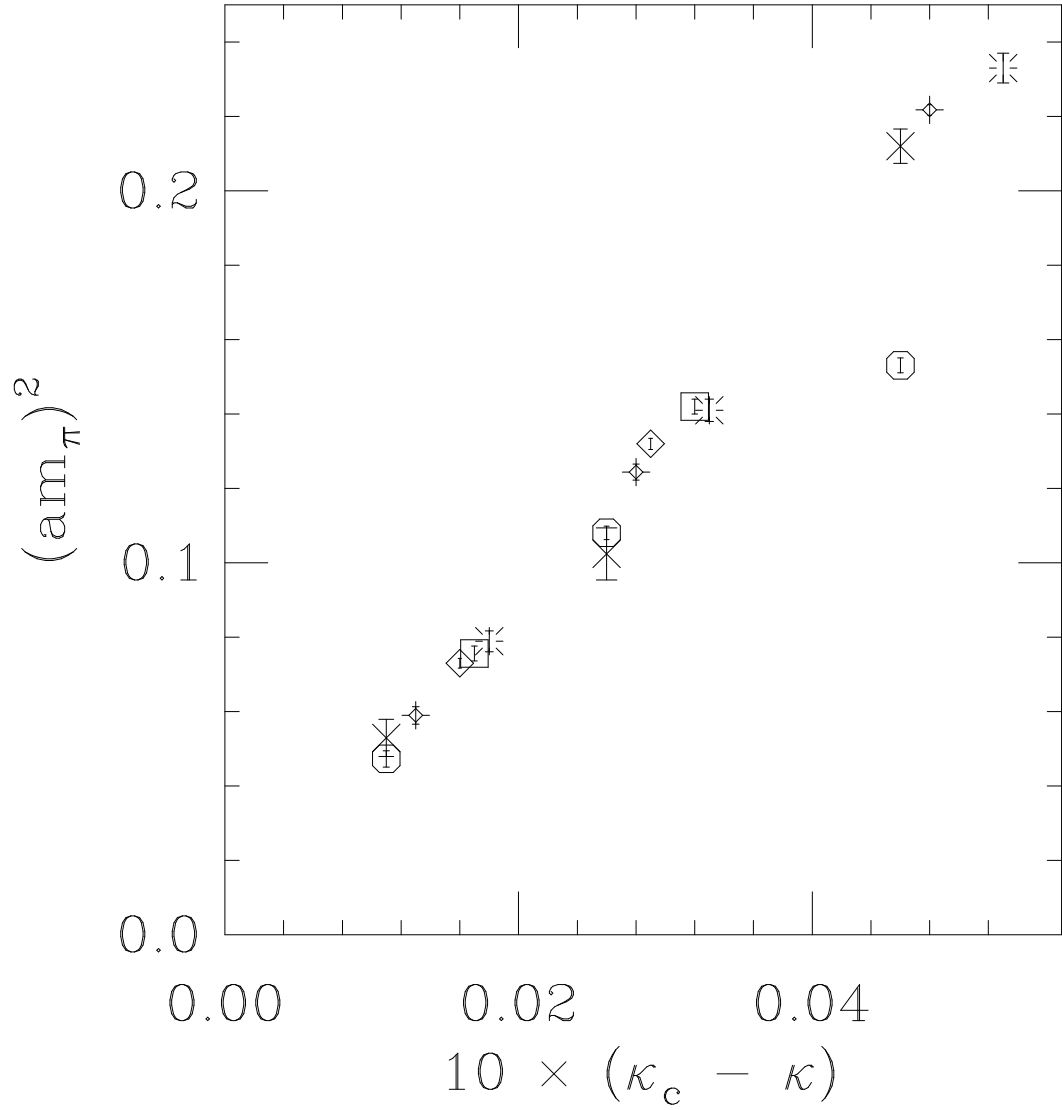


Figure 14: Square of pion mass in lattice units for quenched and dynamical staggered simulations. Data are labelled as in Fig. 13 and the  $16^4 am_q = .025$  dynamical fermion data are labelled by a fancy diamond.

## 4 Conclusions

This concludes our program of spectroscopy for Wilson valence quarks with staggered sea quarks at  $\beta = 5.6$  on  $16^3 \times 32$  lattices. The spectroscopy we see is generally consistent with our earlier results (when performed on lattices of the same spatial volume) and represents an improvement over our previous results insofar as the simulation volume is larger. By comparing results from spatial volumes of  $12^3$  and  $16^3$ , we saw that for the smaller volume baryons with light valence quarks suffer from finite lattice size effect regardless of the dynamical fermion mass we used. This is another piece of evidence which suggests that sea quark properties are much less important than valence quark properties, in the parameter range we have studied. Perhaps we are also seeing the same effect on the pion mass. Of course, one can not be sure that our results are still not contaminated by finite volume effects on  $16^3$  lattices; to test that would require simulations in a larger volume with otherwise unchanged parameter values.

When we compare our spectroscopy with dynamical fermions to quenched results we do not see any dramatic differences. Apparently at the parameter values of the simulation sea quarks simply do not affect spectroscopy above the five to ten per cent level.

However, we have to say that we have always regarded this quark combination as something done as much for expedience as for curiosity. Wilson quarks and staggered quarks have very different symmetries. The next barrier in spectroscopy calculations will occur when lattices become large enough and quark masses become small enough that the rho meson mass falls below the lightest  $I = 1, J = 1 \pi\pi$  state on the lattice, or that the lightest propagating state in the rho channel is a  $\pi\pi$  pair. These pions will each be made of one of the rho meson's valence quark(antiquark) and an antiquark(quark) which has popped out of the sea. It would be desirable if both quark and antiquark have the same internal symmetry structure (for example, one will want to know the mass of the pion in advance), and this argues against further use of "hybrid" quark calculations.

## 5 Acknowledgments

This work was supported by the U. S. Department of Energy under contracts DE-FG02-85ER-40213, DE-AC02-86ER-40253, DE-AC02-84ER-40125, W-31-109-ENG-38, and by the National Science Foundation under grants NSF-PHY87-01775, NSF-PHY89-04035 and NSF-PHY86-14185. The computations were carried out at the Florida State University Supercomputer Computations Research Institute which is partially funded by the U.S. Department of Energy through Contract No. DE-FC05-85ER250000. We thank T. Kitchens and J. Mandula for their continuing support and encouragement.

## References

- [1] For a review of recent progress, see the talk by D. Toussaint in Lattice Gauge Theory '91 (Tsukuba, 1991), Nucl. Phys. B, to appear.
- [2] K. Bitar et al., Phys. Rev. Let. **65**, 2106 (1990), Phys. Rev. **D42**, 3794 (1990).
- [3] A. Krasnitz, Phys. Rev. **D42**, 1301 (1990).
- [4] K. Bitar et al., in the Proceedings of Lattice '90, Nucl. Phys. **B20** (Proc. Suppl), (1991) 362, and in the Proceedings of Lattice '91, Nucl. Phys. **B**, to appear.
- [5] H. C. Andersen, J. Chem. Phys. **72**, 2384 (1980); S. Duane, Nucl. Phys. **B257**, 652 (1985); S. Duane and J. Kogut, Phys. Rev. Let. **55**, 2774 (1985); S. Gottlieb, W. Liu, D. Toussaint, R. Renken and R. Sugar, Phys. Rev. **D35**, 2531 (1987).
- [6] S. Duane, A. Kennedy, B. Pendleton, and D. Roweth, Phys. Let. **194B**, 271 (1987).
- [7] J. E. Mandula and M. C. Ogilvie, Phys. Let. **B248**, 156 (1990).
- [8] Wall sources were first introduced by the APE collaboration and are described by E. Marinari, in the Proceedings of the 1988 Symposium on Lattice Field Theory, A. Kronfeld and P. Mackenzie, eds., Nucl. Phys. **B9** (Proc. Suppl), 209 (1989). Our particular implementation arose through discussions with G. Kilcup.
- [9] T. DeGrand, Comput. Phys. Commun. **52**, 161 (1988).
- [10] C. Liu, in the Proceedings of Lattice '90, Nucl. Phys. **B20** (Proc. Suppl), 149 (1991). A. D. Kennedy, Intl. J. Mod. Phys. **C3**, 1 (1992).
- [11] See, for example, K. C. Bowler, et. al., Nucl. Phys. **B240**, 213 (1984).
- [12] For a discussion of this fitting method see D. Toussaint, in "From Actions to Answers—Proceedings of the 1989 Theoretical Advanced Summer Institute in Particle Physics," T. DeGrand and D. Toussaint, eds., (World, 1990).
- [13] A. DeRujula, H. Georgi, and S. Glashow, Phys. Rev. **D12**, 147 (1975).
- [14] Y. Iwasaki, T. Yoshie, Phys. Let. **B216**, 387 (1989), Y. Iwasaki, in the Proceedings of the 1988 Symposium on Lattice Field Theory, Nucl. Phys. **B9** (Proc. Suppl.), 254 (1989).



kind	$\kappa_{ave}$	$D_{min}$	$D_{max}$	mass	$\chi^2/dof$	C.L.
1 1 (WW)	0.1320	5	16	1.485( 2)	11.390/10	0.328
2 1 (WW)	0.1365	5	16	1.310( 2)	7.417/10	0.686
2 2	0.1410	11	16	1.120( 1)	0.774/4	0.942
3 1 (WW)	0.1422	6	16	1.091( 2)	8.956/9	0.441
3 2	0.1467	11	16	0.894( 1)	0.346/4	0.987
3 3	0.1525	10	16	0.644( 1)	5.312/5	0.379
4 1 (WW)	0.1442	6	16	1.015( 3)	11.067/9	0.271
4 2	0.1487	11	16	0.816( 1)	0.928/4	0.921
4 3	0.1545	10	16	0.552( 1)	7.073/5	0.215
4 4	0.1565	5	16	0.447( 1)	14.519/10	0.151
5 1 (WW)	0.1452	6	16	0.978( 3)	12.355/9	0.194
5 2	0.1497	10	16	0.776( 1)	2.748/5	0.739
5 3	0.1555	5	16	0.502( 1)	14.849/10	0.138
5 4	0.1575	5	16	0.393( 1)	13.308/10	0.207
5 5	0.1585	5	16	0.331( 1)	11.980/10	0.286
6 1 (WW)	0.1460	6	16	0.952( 4)	14.464/9	0.107
6 2	0.1505	10	16	0.748( 2)	2.100/5	0.835
6 3	0.1562	5	16	0.467( 1)	11.694/10	0.306
6 4	0.1583	5	16	0.350( 1)	9.674/10	0.470
6 5	0.1593	5	16	0.280( 2)	7.110/10	0.715
6 6	0.1600	4	16	0.214( 2)	6.099/11	0.867

Table 1: Fits to pseudoscalar mesons, with Wilson valence fermions and  $am_q = 0.01$  staggered sea quarks. All fits are to “kind=1” WP propagators, unless otherwise indicated, and are to a single exponential. In this and following tables, numbers in the “kind” column for mesons refers to their quark content: 1 through 6 refer to hopping parameter .1320, .1410, .1525, .1565, .1585, and .1600.

kind	$\kappa_{ave}$	$D_{min}$	$D_{max}$	mass	$\chi^2/dof$	C.L.
1 1 (WW)	0.1320	5	16	1.493( 2)	9.056/10	0.527
2 1 (WW)	0.1365	5	16	1.321( 2)	7.275/10	0.699
2 2	0.1410	11	16	1.137( 1)	0.591/4	0.964
3 1 (WW)	0.1422	6	16	1.106( 3)	5.972/9	0.743
3 2	0.1467	10	16	0.919( 1)	1.689/5	0.890
3 3	0.1525	6	16	0.688( 1)	6.147/9	0.725
4 1 (WW)	0.1442	6	16	1.030( 3)	5.885/9	0.751
4 2	0.1487	10	16	0.844( 2)	1.565/5	0.905
4 3	0.1545	6	16	0.610( 2)	4.314/9	0.890
4 4	0.1565	8	16	0.526( 3)	5.088/7	0.649
5 1 (WW)	0.1452	6	16	0.993( 4)	5.877/9	0.752
5 2	0.1497	6	16	0.804( 1)	7.780/9	0.556
5 3	0.1555	5	16	0.572( 2)	8.688/10	0.562
5 4	0.1575	8	16	0.485( 3)	6.766/7	0.454
5 5	0.1585	8	16	0.442( 4)	8.550/7	0.287
6 1 (WW)	0.1460	7	16	0.960( 6)	4.150/8	0.843
6 2	0.1505	6	16	0.778( 2)	6.007/9	0.739
6 3	0.1562	5	16	0.546( 3)	13.120/10	0.217
6 4	0.1583	8	16	0.455( 4)	12.455/7	0.087
6 5	0.1593	8	16	0.411( 6)	13.128/7	0.069
6 6	0.1600	11	16	0.391(19)	4.901/4	0.298

Table 2: Fits to vector mesons, with Wilson valence fermions and  $am_q = 0.01$  staggered sea quarks. All fits are to “kind=1” WP propagators, unless otherwise indicated, and are to a single exponential.

kind	$\kappa_{ave}$	$D_{min}$	$D_{max}$	mass	$\chi^2/dof$	C.L.
(WW)	0.1320	7	16	2.327(14)	5.911/8	0.657
	0.1410	11	16	1.777( 3)	4.052/4	0.399
	0.1525	9	16	1.097( 4)	7.926/6	0.244
	0.1565	8	16	0.839( 5)	4.193/7	0.757
	0.1585	8	16	0.699( 8)	3.864/7	0.795
	0.1600	7	16	0.610(23)	8.984/8	0.344

Table 3: Fits to nucleons, with Wilson valence fermions and  $am_q = 0.01$  staggered sea quarks. All fits are to WP propagators, unless otherwise indicated, and are to a single exponential.

kind	$\kappa_{ave}$	$D_{min}$	$D_{max}$	mass	$\chi^2/dof$	C.L.
(WW)	0.1320	7	16	2.331(14)	6.130/8	0.633
	0.1410	11	16	1.786( 3)	4.027/4	0.402
	0.1525	10	16	1.123( 5)	3.768/5	0.583
	0.1565	8	16	0.876( 6)	5.423/7	0.608
	0.1585	5	16	0.743( 6)	11.553/10	0.316
	0.1600	4	16	0.628(10)	4.594/11	0.949

Table 4: Fits to deltas, with Wilson valence fermions and  $am_q = 0.01$  staggered sea quarks. All fits are to “kind=1” WP propagators, unless otherwise indicated, and are to a single exponential.

kind	$\kappa_{ave}$	$D_{min}$	$D_{max}$	mass	$\chi^2/dof$	C.L.
1 1 (WW)	0.1320	5	16	1.500( 2)	13.391/10	0.203
2 1 (WW)	0.1365	5	16	1.328( 2)	12.433/10	0.257
2 2	0.1410	11	16	1.135( 1)	3.975/4	0.409
3 1 (WW)	0.1422	4	16	1.112( 2)	22.669/11	0.020
3 2	0.1467	10	16	0.912( 1)	2.320/5	0.803
3 3	0.1525	8	16	0.664( 1)	1.299/7	0.988
4 1 (WW)	0.1442	9	16	1.047( 4)	16.354/6	0.012
4 2	0.1487	9	16	0.833( 1)	3.820/6	0.701
4 3	0.1545	6	16	0.571( 1)	4.799/9	0.851
4 4	0.1565	5	16	0.470( 1)	5.376/10	0.865
5 1 (WW)	0.1452	4	16	0.999( 2)	27.140/11	0.004
5 2	0.1497	8	16	0.794( 1)	4.970/7	0.664
5 3	0.1555	6	16	0.524( 1)	3.550/9	0.938
5 4	0.1575	4	16	0.417( 1)	6.493/11	0.839
5 5	0.1585	4	16	0.358( 1)	8.052/11	0.709
6 1 (WW)	0.1460	4	16	0.968( 2)	20.236/11	0.042
6 2	0.1505	7	16	0.764( 1)	6.954/8	0.542
6 3	0.1562	5	16	0.488( 1)	5.677/10	0.842
6 4	0.1583	4	16	0.375( 1)	7.843/11	0.727
6 5	0.1593	4	16	0.310( 1)	12.291/11	0.342
6 6	0.1600	6	16	0.249( 2)	8.813/9	0.455

Table 5: Fits to pseudoscalar mesons, with Wilson valence fermions and  $am_q = 0.025$  staggered sea quarks. All fits are to “kind=1” WP propagators, unless otherwise indicated, and are to a single exponential.

kind	$\kappa_{ave}$	$D_{min}$	$D_{max}$	mass	$\chi^2/dof$	C.L.
1 1 (WW)	0.1320	5	16	1.510( 2)	12.381/10	0.260
2 1 (WW)	0.1365	5	16	1.340( 2)	12.593/10	0.247
2 2	0.1410	10	16	1.153( 1)	4.781/5	0.443
3 1 (WW)	0.1422	4	16	1.129( 2)	16.722/11	0.116
3 2	0.1467	9	16	0.939( 1)	3.797/6	0.704
3 3	0.1525	7	16	0.716( 1)	4.054/8	0.852
4 1 (WW)	0.1442	4	16	1.056( 2)	17.731/11	0.088
4 2	0.1487	9	16	0.867( 1)	3.451/6	0.750
4 3	0.1545	6	16	0.638( 2)	6.693/9	0.669
4 4	0.1565	6	16	0.560( 2)	8.757/9	0.460
5 1 (WW)	0.1452	4	16	1.019( 2)	14.718/11	0.196
5 2	0.1497	7	16	0.830( 1)	5.110/8	0.746
5 3	0.1555	6	16	0.601( 2)	8.517/9	0.483
5 4	0.1575	8	16	0.520( 3)	7.019/7	0.427
5 5	0.1585	4	16	0.483( 3)	15.228/11	0.172
6 1 (WW)	0.1460	4	16	0.991( 3)	9.075/11	0.615
6 2	0.1505	7	16	0.805( 2)	3.556/8	0.895
6 3	0.1562	8	16	0.574( 3)	3.806/7	0.802
6 4	0.1583	8	16	0.494( 4)	5.101/7	0.648
6 5	0.1593	4	16	0.458( 3)	14.068/11	0.229
6 6	0.1600	4	16	0.434( 5)	12.901/11	0.300

Table 6: Fits to vector mesons, with Wilson valence fermions and  $am_q = 0.025$  staggered sea quarks. All fits are to “kind=1” WP propagators, unless otherwise indicated, and are to a single exponential.

kind	$\kappa$	$D_{min}$	$D_{max}$	mass	$\chi^2/dof$	C.L.
(WW)	0.1320	5	16	2.364(10)	9.873/10	0.452
(WW)	0.1410	5	16	1.833(10)	7.799/10	0.649
	0.1525	10	16	1.139( 5)	6.934/5	0.226
	0.1565	6	16	0.878( 4)	9.811/9	0.366
	0.1585	6	16	0.744( 6)	8.209/9	0.513
	0.1600	6	16	0.642(12)	5.432/9	0.795

Table 7: Fits to nucleons, with Wilson valence fermions and  $am_q = 0.025$  staggered sea quarks. All fits are to WP propagators, unless otherwise indicated, and are to a single exponential.

kind	$\kappa_{ave}$	$D_{min}$	$D_{max}$	mass	$\chi^2/\text{dof}$	C.L.
(WW)	0.1320	5	16	2.368(10)	8.734/10	0.558
(WW)	0.1410	5	16	1.844(11)	6.451/10	0.776
	0.1525	10	16	1.164( 6)	3.366/5	0.644
	0.1565	6	16	0.918( 6)	9.785/9	0.368
	0.1585	6	16	0.804(10)	8.522/9	0.483
	0.1600	4	16	0.711( 9)	8.337/11	0.683

Table 8: Fits to deltas, with Wilson valence fermions and  $am_q = 0.025$  staggered sea quarks. All fits are to “kind=1” WP propagators, unless otherwise indicated, and are to a single exponential.

kind	$\kappa_{ave}$	$D_{min}$	$D_{max}$	mass ratio	$\chi^2/\text{dof}$	C.L.
(WW)	0.1320	12	16	0.997( 3)	8.990/6	0.174
	0.1410	11	16	0.985( 1)	2.994/8	0.935
	0.1525	11	16	0.933( 2)	6.317/8	0.612
	0.1565	11	16	0.853( 5)	10.740/8	0.217
	0.1585	11	16	0.752(11)	11.370/8	0.182
	0.1600	11	16	0.558(27)	5.007/8	0.757

Table 9: Fits to the ratio  $m_\pi/m_\rho$ , with Wilson valence fermions and  $am_q = 0.01$  staggered sea quarks. All fits are to “kind=1” WP propagators, unless otherwise indicated, and are correlated fits to a single exponential in each channel.

kind	$\kappa$	$D_{min}$	$D_{max}$	mass ratio	$\chi^2/\text{dof}$	C.L.
(WW)	0.1320	7	16	1.563( 8)	11.600/16	0.771
	0.1410	11	16	1.563( 3)	4.961/8	0.762
	0.1525	8	16	1.590( 5)	12.880/14	0.536
	0.1565	7	16	1.591(11)	12.520/16	0.707
	0.1585	8	16	1.597(30)	17.370/14	0.237
	0.1600	6	16	1.573(53)	39.600/18	0.002

Table 10: Fits to the ratio  $m_N/m_\rho$ , with Wilson valence fermions and  $am_q = 0.01$  staggered sea quarks. All fits are to “kind=1” WP propagators, unless otherwise indicated, and are correlated fits to a single exponential in each channel.

kind	$\kappa_{ave}$	$D_{min}$	$D_{max}$	mass ratio	$\chi^2/\text{dof}$	C.L.
(WW)	0.1320	13	16	1.002( 5)	14.510/4	0.006
(WW)	0.1410	6	16	0.984( 2)	25.800/18	0.104
	0.1525	11	16	0.984( 1)	3.694/8	0.884
	0.1565	7	16	0.929( 1)	7.176/16	0.970
	0.1585	7	16	0.845( 3)	14.150/16	0.588
	0.1600	8	16	0.744( 7)	14.560/14	0.409

Table 11: Fits to  $m_\pi/m_\rho$ , with Wilson valence fermions and  $am_q = 0.025$  staggered sea quarks. All fits are to “kind=1” WP propagators, unless otherwise indicated, and are correlated fits to a single exponential in each channel.

kind	$\kappa_{ave}$	$D_{min}$	$D_{max}$	mass ratio	$\chi^2/\text{dof}$	C.L.
(WW)	0.1320	6	16	1.564( 8)	23.060/18	0.188
(WW)	0.1410	5	16	1.584( 9)	30.380/20	0.064
	0.1525	11	16	1.568( 2)	8.207/8	0.414
	0.1565	11	16	1.596( 5)	5.214/8	0.734
	0.1585	6	16	1.553( 9)	21.590/18	0.251
	0.1600	6	16	1.516(15)	21.200/18	0.269

Table 12: Fits to  $m_N/m_\rho$ , with Wilson valence fermions and  $am_q = 0.025$  staggered sea quarks. All fits are to “kind=1” WP propagators, unless otherwise indicated, and are correlated fits to a single exponential in each channel.

$am_q$	particle	mass
0.01	$\rho$	.360(8)
	p	.524(18)
	$\Delta$	.560(12)
0.025	$\rho$	.386(5)
	p	.558(12)
	$\Delta$	.651(17)

Table 13: Extrapolations to  $\kappa_c$ .

kind	$\kappa_{ave}$	$D_{min}$	$D_{max}$	mass	$\chi^2/dof$	C.L.
pion	0.1585	7	16	0.378( 2)	12.382/8	0.135
	0.1600	7	16	0.273( 3)	12.821/8	0.118
rho	0.1585	8	16	0.530( 6)	2.857/7	0.898
	0.1600	7	16	0.486( 9)	5.388/8	0.715
proton	0.1585	7	16	0.783(10)	8.339/8	0.401
	0.1600	6	16	0.673( 9)	8.113/9	0.523
delta	0.1585	8	16	0.852(11)	9.302/7	0.232
	0.1600	8	16	0.757(25)	3.628/7	0.821

Table 14: Fits to quenched  $\beta = 5.85$  spectroscopy with Wilson valence fermions. All fits are to a single exponential.

kind	$\kappa_{ave}$	$D_{min}$	$D_{max}$	mass	$\chi^2/dof$	C.L.
pion	0.1554	7	16	0.362( 1)	5.284/8	0.727
	0.1567	7	16	0.271( 2)	10.564/8	0.228
rho	0.1554	5	16	0.486( 3)	13.433/10	0.200
	0.1567	4	16	0.445( 5)	19.847/11	0.047
proton	0.1554	6	16	0.721( 6)	11.226/9	0.261
	0.1567	6	16	0.619( 8)	4.814/9	0.850
delta	0.1554	6	16	0.777( 7)	12.580/9	0.183
	0.1567	6	16	0.699( 9)	7.574/9	0.578

Table 15: Fits to quenched  $\beta = 5.95$  spectroscopy with Wilson valence fermions. All fits are to a single exponential.

kind	$\kappa$	$D_{min}$	$D_{max}$	mass ratio	$\chi^2/dof$	C.L.
$m_\pi/m_\rho$	0.1585	7	16	0.716( 6)	11.050/16	0.806
	0.1600	7	16	0.573(10)	11.740/16	0.762
$m_N/m_\rho$	0.1585	7	16	1.468(16)	8.603/16	0.929
	0.1600	5	16	1.415(24)	15.060/20	0.773

Table 16: Fits to ratios  $m_\pi/m_\rho$  and  $m_N/m_\rho$ , from quenched  $\beta = 5.85$  simulations with Wilson valence fermions. All fits are to “kind=1” WP propagators, and are correlated fits to a single exponential in each channel.

kind	$\kappa_{ave}$	$D_{min}$	$D_{max}$	mass ratio	$\chi^2/\text{dof}$	C.L.
$m_\pi/m_\rho$	0.1554	10	16	0.740( 8)	5.786/10	0.833
	0.1567	10	16	0.599(16)	7.037/10	0.722
$m_N/m_\rho$	0.1554	10	16	1.507(27)	7.394/10	0.688
	0.1567	4	16	1.420(18)	24.370/22	0.328

Table 17: Fits to ratios  $m_\pi/m_\rho$  and  $m_N/m_\rho$ , from quenched  $\beta = 5.95$  simulations with Wilson valence fermions. All fits are to “kind=1” WP propagators, and are correlated fits to a single exponential in each channel.